IGS-20

Model tests on the stability of GRS integral bridge against tsunami load

Shohei Kawabe [i)], Yoshiaki Kikuchi [ii)], Kenji Watanabe [iii)] and Fumio Tatsuoka [iv)]

i) Researcher, Facilities and Geotechnical Engineering Research Division, National Institute for Rural Engineering, 2-1-6, Kannondai, Tsukuba City 305-8609, Japan.
ii) & iv) Professor, Department of Civil Engineering, Tokyo University of Science, 2641, Yamazaki, Noda City 278-8510, Japan.
iii) Senior Researcher, Structure Technology Division, Railway Technical Research Institute, 2-8-38, Hikari-cho, Kokubunji City 185-8540, Japan.

ABSTRACT

The girders of a great number of bridges were washed away and/or their approach fills were significantly eroded by the great tsunami of the 2011 Great East Japan Earthquake. Many of the bridges close to coastal lines are required to have high resistance against not only seismic load but also tsunami load. The geosynthetic-reinforced soil integral bridge (GRS-IB) has been developed and it has been verified that this new type bridge has high seismic stability. This paper reports results of small scale hydraulic model tests showing substantially higher stability against tsunami load of GRS-IB than the conventional type bridge, having a girder supported by bearings. This high performance can be attributed to the fact that the girder, the abutments (i.e., facings) and the approach fills of GRS-IB are structurally integrated to each other. Accordingly the resistance of the backfill against erosion is also very high.

Keywords: earthquake, tsunami, erosion, geosynthetic-reinforced soil integral bridge, model test

1. INTRODUCTION

A great number of bridges were seriously damaged by the 2011 Great East Japan Earthquake. Although some of them were damaged by pro-longed strong seismic motions, most of them (i.e., more than 340 bridges; Kosa 2012) was collapsed by the great tsunami immediately after the earthquake. With these bridges, the girders were washed away and/or the approach fills were significantly eroded by tsunami currents. Many bridges that have been or will be constructed close to coastal lines are required to have high resistance against not only seismic load but also tsunami load.

Tatsuoka et al. (2007, 2015) developed a new bridge type, called Geosynthetic-Reinforced Soil Integral Bridge (GRS-IB) (Fig. 1). GRS-IB is constructed as follows: 1) a pair of approach fills of geosynthetic-reinforced backfill are constructed; 2) a pair of full-height rigid (FHR) facing are constructed by casting-in-place concrete on the geogrid-wrapped-around wall face firmly connecting the geogrid reinforcement to the facing; and 3) a girder is constructed with both ends structurally integrated to the top of the facings.

Aizawa et al. (2007) and Hirakawa et al. (2007), among others, performed a series of shaking table model tests to show that GRS-IB has much higher seismic stability than the conventional type bridge comprising a simple-supported girder supported by bearings. Koda et al. (2013) confirmed the above by performing full-scale model tests. Tatsuoka et al. (2015) showed that the construction and maintenance cost of GRS-IB is much lower than the conventional type bridge under otherwise the same conditions.

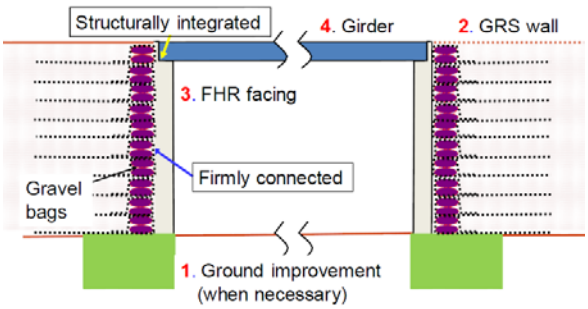

Fig. 1. GRS-IB; the numbers show the construction sequence.

So far, one prototype GRS-IB was completed in 2012 for a new high-speed train line in Hokkaido and three others to restore the bridges of Sanriku Railway that were fully collapsed by the great tsunami of the 2011 Great East Japan Earthquake. Several others are at the stage of design or construction.

This paper reports the result of small scale hydraulic model tests on GRS-IB, as well as the conventional type bridge, to find whether GRS-IB has high stability against tsunami load due to structural integration of the girder, facings and approach fills.

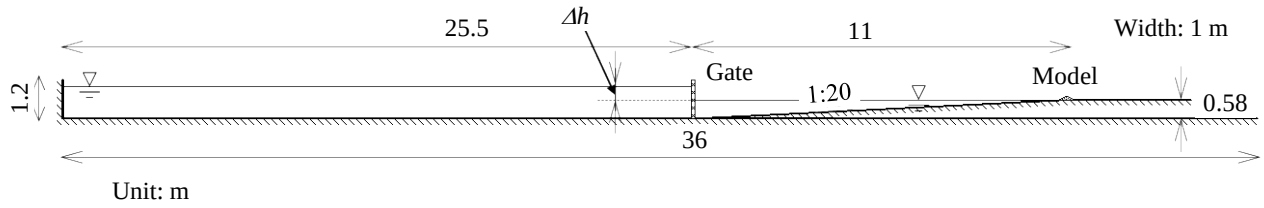

Fig. 2. Open channel used in this study.

2 GENERAL SPECIFICATIONS

Small scale bridge models were placed in an open channel (Fig. 2) and subjected to a series of hydraulic bore as modelled tsunami. The scaling factors employed in this study are listed in Table 1. The scaling factors other than those for length, density and acceleration were obtained by assuming that the Froude number at the crest of the model embankment is equal to 1.0.

Table 1. Similitude of the model test.

Items	Scaling factors (prototype/model)
Length	λ (assumed to be equal to 80)
Froude number	1.0 at the crest of the model
Density	1.0
Acceleration	1.0
Velocity	$\lambda^{0.5}$
Time	$\lambda^{0.5}$
Pressure, Stress	λ
Force	λ^3

2.1 Channel and hydraulic bore

Hydraulic bores were made by suddenly opening a gate at the middle of the open channel (Fig. 2) arranged to produce a difference in the water level Δh between the opposite sides. The wave of hydraulic bore climbed up a gentle slope in front of the model bridge located on the horizontal channel floor. The wave was broken before reaching the model. The test cases are listed in Table 2. The overflow depth is defined at the center of the crest of the model embankment (Fig. 3). Two models were tested, the conventional type bridge (case 01) and GRS-IB (case 02). When the damage to the model by a given wave was not serious, another wave with a larger overflow depth was applied in the sequence shown in Table 2. The model of GRS-IB did not collapsed even by the largest wave applied in this study.

Table 2. List of tests.

Case	Bridge type	Δh (cm)	Approximate overflow depth in model scale (cm)
01-1	Conventional	30	10
01-2		40	15
02-1	GRS-IB	30	10
02-2		40	15
02-3		50	20
02-4		50	20

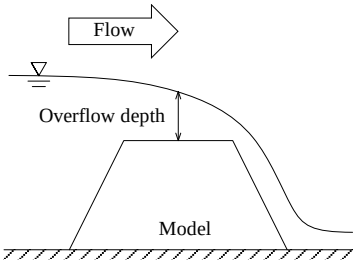

Fig. 3. Definition of the overflow depth.

2.2 Bridge models

Fig. 4 shows the whole of the model of GRS-IB. The model embankment was constructed by compacting a poorly graded fine sand (Toyoura sand, e_{min} = 0.62, e_{max} = 0.97) at the optimum water content (i.e. 15.2 %) to a relative density D_r = 85 %. The panels covering the steep slopes and crest were made by cutting a 5 mm-thick duralumin plates. The model geogrid (Fig. 5) was made by cutting a net of polyester and polyvinyl chloride with an aperture of 4 mm.

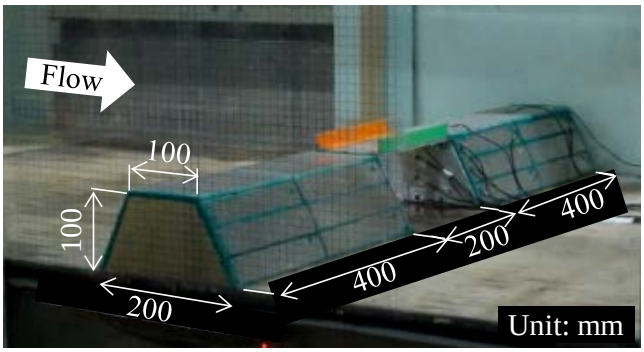

Fig. 4. Model of GRS-IB.

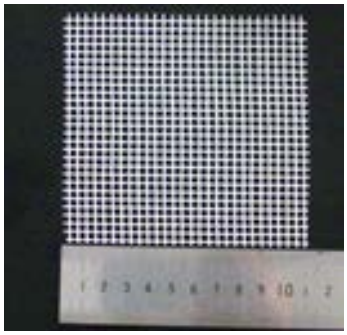

Fig. 5. Model geogrid.

The model geogrid reinforcement layers were connected to the back faces of the panels on the slope and the abutments (facings) by using bolts and stainless steel strips. The connection between the geogrid layers and the slope panels and facings was made strong enough not to rupture during the test. The panels on the crest of the embankment were connected to those on the sea side slopes. The girder and facings were also made of 5 mm-thick duralumin plates. The facings had no footing. The girder was integrated to the crest of the abutments (facings) by using bolts.

Fig. 6 shows the whole of the model of the conventional type bridge. The model was made in the similar way as the model of GRS-IB except for the followings. The slope of the embankment was much gentler than the model of GRS-IB, while the backfill was not geogrid-reinforced and the covering panels were simply placed on the slopes and crest of the embankment. The girder was placed on the crest of the bridge abutments (Fig. 7). A footing was arranged at the heel of the abutment as the prototype of conventional type bridge so that the model abutment can be stable against earth pressure and other external loads. Note that the facing of the model of GRS-IB had no such a footing.

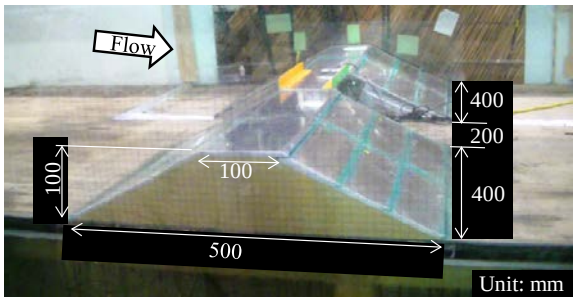

Fig. 6. Model of conventional type bridge.

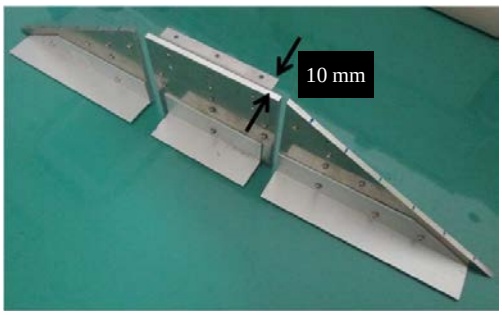

Fig. 7. Back side view of the abutment of conventional type bridge model.

The two bridge models were placed on the rigid floor of the channel (Fig. 2). The gap between the end faces of the model embankment and the side walls of the channel was sealed by using silicon grease.

2.3 Measurements of earth and water pressures

Wave pressure and earth pressure were measured by using small disk-type pressure transducers with 0.6 mm in thickness and 6 mm in diameter. They were glued on the model as shown in Fig. 8.

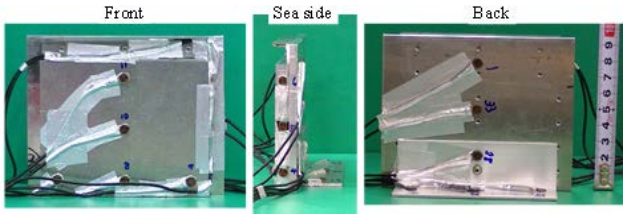

Fig. 8. Pressure sensors placed on the abutment of conventional type bridge model.

3 TIEST RESULTS

Movies of the model tests were taken by multiple digital video cameras. Some typical observations from these movies and pressure measurements are reported below.

3.1 Collapse process from movies

In case 01 on the conventional type bridge, two waves were applied. The girder was washed away by the first wave. As the damage to the abutment and backfill was not noticeable, the second wave was applied consecutively to the model that had lost the girder. The panel immediately behind the abutment on the crest of the embankment (i.e., the one on the right side in Fig. 9) was washed away only two seconds after the start of over flowing of the wave current. Then, erosion and washing away of the backfill material started, followed by continuous erosion of the backfill. Ultimately, the panels on the slopes and the abutments were washed away. This result indicates that the weak points against tsunami current of the conventional type bridge are the girder bearings, the panels on the slopes and the unreinforced backfill. That is, this unstable behaviour is due to the fact that the members of the bridges (i.e., the girder, the abutments, the panels and the approach fills) are not integrated to each other.

Fig. 9. During overflow in case 01-2.

In case 02 on the GRS-IB model, any noticeable damage by the first wave was not observed. After the second wave, which caused extensive damage to the conventional type bridge model, and even after the third wave, the damage was not noticeable. Therefore, the fourth wave was applied. In this case, the structural damage to the bridge members was negligible.

However, three seconds after the start of overflow, the model started deforming to an arch shape by a force of this wave, as shown in Fig. 10. The two broken lines shown in Fig. 10 indicate the initial locations of the toes of the slopes. This deformation of the model continued during subsequent steady state overflow. It was also observed that a small amount of the backfill material was eroded and washed away.

Fig. 10. After fourth wave in case 02-4.

One of the characteristics features of GRS structures is high stability despite of such steep slopes that unreinforced embankment cannot be stable. Steep-sloped embankment requires smaller earthwork and occupies smaller land. Then, steep-sloped reinforced embankment is usually more cost-effective than conventional gentle-sloped unreinforced embankment. In view of the above, the slope of the approach fills of the GRS-IB model (Fig. 4) was made much steeper than that of the conventional type bridge model (Fig. 6). However, the steep-sloped reinforced embankment has the following two drawbacks: 1) a reduction in the resistance against the lateral impact of tsunami current due to a reduction of the total weight; and 2) an increase in the impact of tsunami on the upstream slope due to an increased slope. As a result, such deformation as seen in Fig. 10 becomes likely to take place. This issue will be studied in the future taking into account the actual magnitude and continuing time of the devastating tsunami current.

It seems that the internal erosion of backfill took place after the start of the deformation seen in Fig. 10 started. Fig. 11 shows the soil layers overlying the respective geogrid layers observed when dismantling the model from the top after test case 02-4. The eroded area are enclosed in red line. The backfill in the three layers from the top were noticeably eroded, but less in the lower layers. The bottom layer was not eroded. This performance is substantially better than the conventional type bridge model (case 01) and can be attributed to the fact that the panels on the slopes and crest of the embankment survived the waves because of connection of the panels and abutment facings to the geogrid layers reinforcing the backfill. Such an effective suppression of backfill erosion as observed in case 02 eventually increased the stability of the abutment facings and girder of GRS-IB, thus the stability of the whole of the structure.

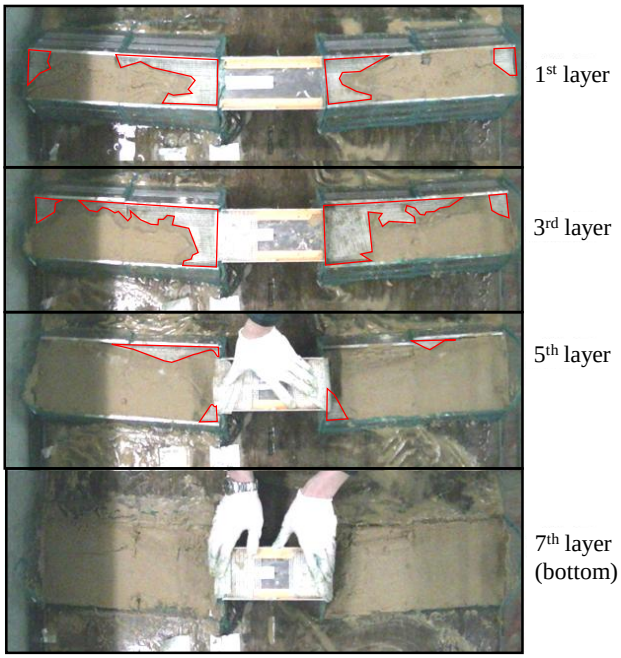

Fig. 11. Erosion of the backfill observed after test case 02-4.

3.2 Water and earth pressures

Figs. 12 and 13 show the time histories of water and earth pressures by the first wave measured in test cases 01 and 02. These are typical of all the measurements in this study. In test case 01-1 (Fig. 12), the erosion of backfill was very limited despite the washing away of the girder. The water and earth pressures acting on the abutment presented in Fig. 12 were essentially free from the effects of the girder. In these figures, the horizontal (time) axis was set zero at the time when the wave arrived at the sea side slope of the embankment. Before this moment, the water pressure were essentially zero and set zero at the time of wave arrival. The earth pressures shown in these figures are the increment from the values before the wave arrival. In both tests, the duration of the overflow of wave was around ten seconds. The names shown in these figures, P01 - P54, denote the positions of the sensors.

The following trends of behaviour may be seen from Fig. 12 for the conventional type bridge model. Firstly, the impact water pressure at P03, near the bottom of the upstream slope of the abutment, was about 5 kN/m^2 (Fig. 12a). In comparison, the water pressure at the subsequent steady state during the overflow was much lower and rather constant while similar to the hydrostatic pressure. The water pressure acting on the front face of the abutment in the direction of bridge axis is also similar to the hydrostatic pressure (Fig. 12b). The water pressures at the abutment bottom along the abutment width (P41, P13 & P43) are rather similar. Secondly, the overburden earth pressure on the top face of the heel of the footing of the abutment (P31, P32 & P33) largely fluctuated in the flow direction (Fig. 12c). Yet, these overburden pressures are generally much larger than the lateral earth pressures acting on the back

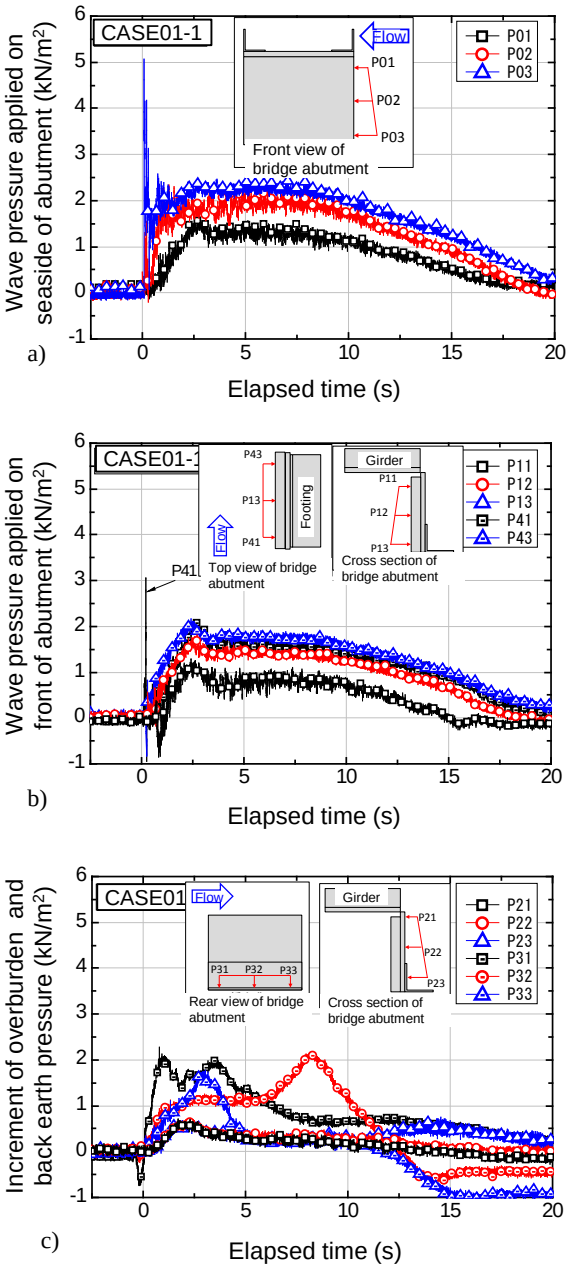

Fig. 12. Test case 01-1 on conventional type bridge model; a) wave pressure applied on seaside of abutment, b) wave pressure applied on the front face of abutment, c) increment of overburden and earth pressure applied on the back face of abutment.

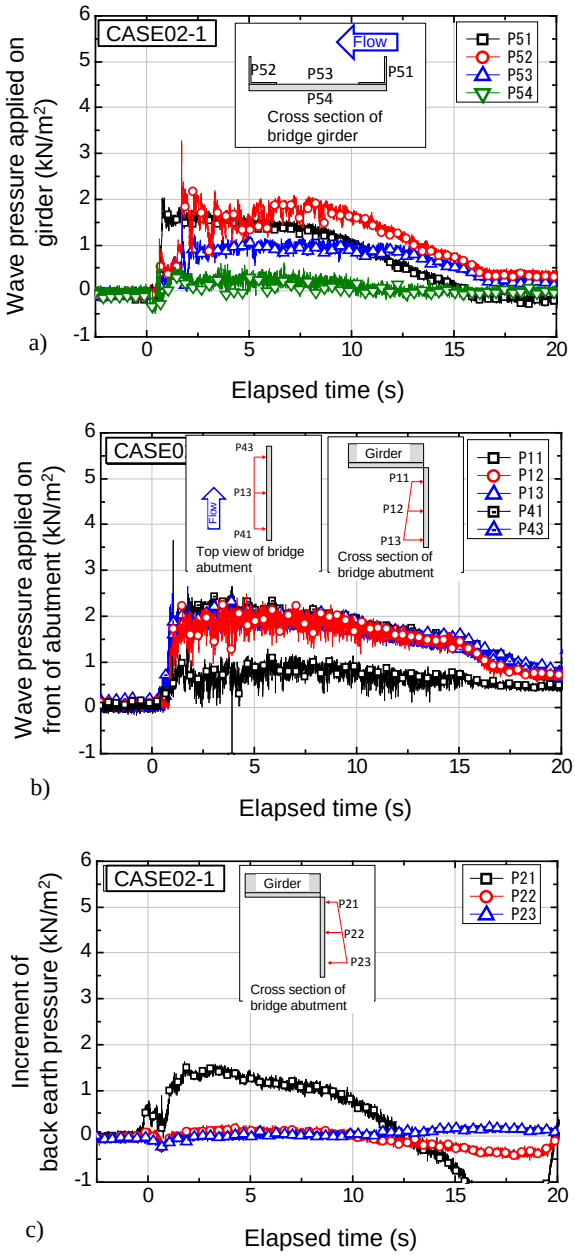

Fig. 13. Test case 02-1 on GRS-IB model; a) wave pressure applied on bridge girder, b) wave pressure applied on the front face of abutment, c) increment of back earth pressure applied on the back face of abutment.

face of the abutment (P21 & P22). This large increase in the overburden earth pressure on the footing heel was due likely to an increase in the water pressure at the crest of embankment that was transmitted towards the bottom of embankment.

The following trends may be seen from Fig. 13 for the GRS-IB model. Firstly, Fig. 13a shows the water pressure acting on the girder. The horizontal load developed by this water pressure was about 2.2 times as large as the total submerged weight of the girder and two abutments, W_t' = about 8.2 N·(1.0 − 1.0/2.79) ≈ 5.26 N, where 2.79 g/cm^3 is the density of the duralumin. Moreover, the horizontal load by the wave pressure acting on the upstream face of the abutment reaches about $0.3W_t'$. So the total lateral wave load is about $2.5W_t'$. On the other hand, the friction angle at the bottom of abutment is very low (about 0.5). Therefore, the frictional resistance at the base of the abutments is about $0.5W_t'$, which is much lower than total wave load. This means that large part of the wave load applied to the girder should have been supported by the weight of the reinforced backfill. Similar data of

the wave pressure acting on the girder could not be obtained in test case 01, because the girder was washed away immediately after the wave arrival. Secondly, Fig. 13b shows the water pressure acting on the front face of the abutment facing in the direction of bridge axis. A relatively large noise in the measurements at P11 and P12, located close to the girder, might be due to unstable streamlines around the girder. These water pressures are similar to those shown in Fig. 12b and similar to the hydrostatic pressure. Thirdly, Fig. 13c shows the earth pressures acting on the back face of the facing in the direction of bridge axis. A very low increase at P22 and P23 may indicates that the abutment facings were very stable against the wave load. On the other hand, the value at P21, located close to the girder, increased significantly. It is likely that the displacement of the girder by wave load was highly restrained at the location of P21 by the facing and reinforced backfill together, then the earth pressure at P21 responded sensitively to potential displacements of the girder. That is, this trend at P21 indicates a high structural integrity of the GRS-IB model contributing to high stability against tsunami current.

4 SUMMARY

The following conclusions can be derived from the small hydraulic model tests performed to evaluate the stability of GRS-IB against tsunami described above:

1) The conventional type bridge is highly vulnerable to strong tsunami load due to low stability of the girder at bearings placed on the top of the abutments and low resistance of the backfill against erosion as a result of low resistance of panels placed on the slopes and crest of the unreinforced embankment.
2) GRS-IB has the following advantageous features in resisting against strong tsunami load:
   a) As the girder and abutment facing are structurally integrated to each other, the girder is stable as long as the abutment facing is stable.
   b) The total weight of the girder and abutment facings may be insufficient to survive strong tsunami load. However, as the abutment facings and approach fills are integrated to each other by geogrid reinforcement layers and the approach fills are rather heavy, the abutment is stable as long as the geogrid reinforcement and its connection to the facing are not ruptured and the backfill is not eroded.
   c) The backfill is stable against erosion from the slope face as long as the panels covering the slopes and crest are stable.
   d) The panels covering the slopes are very stable, as they are connected to the geogrid layers reinforcing the backfill and the panels on the crest are connected to those on the slopes.
   e) As the abutment facing is relatively thin as a result of structural integration to the girder and approach fill, the tsunami load acting on its upstream face is relatively low.
3) When the slope of the geogrid-reinforced approach fills is made steep as in this study, a decrease in their stability against lateral sliding associated with a decrease in the weight should be examined.
4) Even when the backfill is geogrid-reinforced, the joints between adjacent panels and between panels and the abutment facings should be tightly sealed as much as possible to reduce the amount of internal erosion and washed away of the backfill.

ACKNOWLEDGEMENTS

This work was supported by JSPS KAKENHI Grant Number 26820193. The experiments described in this paper were carried out in the open channel of Hydraulic Laboratory, Tokyo University of Science. The authors are grateful to their cooperation.

REFERENCES

1) Aizawa, H., Nojiri, M., Hirakawa, D., Nishikiori, H., Tatsuoka, F., Tateyama, M. and Watanabe, K. (2007): Validation of high seismic stability of A new type integral bridge consisting of geosynthetic-reinforced soil walls, *Proceedings of 5th International Symposium on Earth Reinforcement* (*IS Kyushu 2007*), 819-825.
2) Hirakawa, D., Nojiri, M., Aizawa, H., Nishikiori, H., Tatsuoka, F., Tateyama, M. and Watanabe, K. (2007): Effects of the tensile resistance of reinforcement embedded in the backfill on the seismic stability of GRS integral bridge, *Proceedings of 5th International Symposium on Earth Reinforcement* (*IS Kyushu* 2007), 811-817.
3) Koda, M., Nonaka, T., Suga, M., Kuriyama, M., Tateyama, M. and Tatsuoka, F. (2013): A Series of Lateral Loading Tests on a Full-Scale Model of Geosynthetic-Reinforced Soil Integral Bridge" *Proceedings of International Symposium on Design and Practice of Geosynthetic-Reinforced Soil Structures, Bologna, Italy* (Ling et al., eds.), 157-174.
4) Kosa, K. (2012): Damage analysis of bridges affected by tsunami due to Great East Japan Earthquake, *Proceedings of International Symposium on Engineering Lessons Learned from the 2011 Great East Japan Earthquake*, March, Tokyo, Japan, 1386-1397.
5) Tatsuoka, F., Hirakawa, D., Nojiri, M. & Aizawa, H., Tateyama, M. and Watanabe, K. (2007): A New Type Integral Bridge Comprising of Geosynthetic-Reinforced Soil Walls, *Proceedings of 5th International Symposium on Earth Reinforcement* (*IS Kyushu* 2007), 803-809.
6) Tatsuoka, F., Tateyama, M., Koda, M. Kojima, K., Yonezawa, T., Shindo, Y. and Tamai, S. (2015): Recent research and practice of GRS integral bridges for railways in Japan, *Proceedings of 15th Asian Regional Conference on Soil Mechanics and Geotechnical Engineering, Fukuoka* (to appear in this conference),
7) Yamaguchi, S., Kawabe, S., Watanabe, K., Kikuchi, Y., Nihei, Y. and Tatsuoka, F. (2014): Study on stability of the GRS integral bridge against Tsunami overflow, *Proceedings of special symposium on Great East Japan Earthquake by Japanese Geotechnical Society*, 678-684 (in Japanese).